

Dynamical screening in bilayer graphene

O. V. Gamayun*

Bogolyubov Institute for Theoretical Physics, 14-b Metrologichna Street, Kiev 03680, Ukraine

(Received 11 April 2011; published 22 August 2011)

We calculate one-loop polarization in bilayer graphene in the four-band approximation for arbitrary values of frequency, momentum, and doping. At low and high energy our results reduce to the polarization functions calculated in the two-band approximation and in the case of single-layer graphene, respectively. The special cases of static screening and plasmon modes are analyzed.

DOI: [10.1103/PhysRevB.84.085112](https://doi.org/10.1103/PhysRevB.84.085112)

PACS number(s): 73.22.Pr

I. INTRODUCTION

Graphene, a one-atom-thick layer of graphite, has attracted a lot of attention from both theoreticians and experimentalists since its fabrication.¹ Quasiparticle excitations in graphene have a linear dispersion at low energies and are described by the massless Dirac equation in $2 + 1$ dimensions. Theoretically such behavior was predicted long ago,² and its numerous consequences were experimentally checked after the discovery of graphene in the laboratory.

In contrast to the case of single-layer graphene (SLG), low-energy excitations of the bilayer graphene (BLG) have a parabolic spectrum, although the chiral form of the effective two-band Hamiltonian persists because the sublattice pseudospin is still a relevant degree of freedom. This changes many electronic properties of the material (for a review, see Refs. 3 and 4) compared to the case of monolayer graphene. However, the low-energy approximation in bilayer graphene is valid only for small doping $n < 10^{12} \text{ cm}^{-2}$, while experimentally doping can attain ten times larger densities. For such a large doping, the four-band model⁵ should be used instead of the low-energy effective two-band model.

In the literature, the screening effects in bilayer graphene have mainly been reported within the low-energy effective two-band model^{6,7} and in the presence of a magnetic field.^{8,9} Dynamical polarization plays an important role for finding plasmon excitations as well as for studying the gap equation and excitonic condensates in both single-layer^{10,11} and bilayer graphene.^{7,9} Some attempts to obtain analytical results in the four-band model for bilayer graphene were reported in Refs. 12–14. An exact calculation of the polarization function in the four-band model is interesting also from the purely theoretical viewpoint, because then we can see how the known results for the SLG (Refs. 15 and 16) and the two-band BLG (Ref. 17) are recovered as limiting cases.

Recently, a lot of attention has been paid to investigation of the properties of the polarization operator in SLG.^{18–22} The most general expression for dynamical polarization of SLG at finite temperature, chemical potential, constant impurity rate, quasiparticle gap, and magnetic field is given in Ref. 23.

In this paper, we calculate the BLG dynamical polarization in the four-band model within the random phase approximation (RPA) for arbitrary wave vector, frequency, and doping. Our results can be considered as an extension of the results obtained in Ref. 13, although those results were obtained in a slightly different approach. In Sec. II we describe the model used and present our main result for the polarization function.

We consider in Sec. III A the static polarization function and compare it with the corresponding SLG and two-band BLG results. In Sec. III B we focus on the long-wavelength limit and study plasmons. Finally, we provide the details of our calculations in the Appendix.

II. RPA CALCULATION

We model BLG in the Bernal stacking arrangement,⁵ where for two hexagonal lattices one sublattice of the bottom layer is a near neighbor of the opposite sublattice of the top layer. In the tight-binding approximation, we have the following Hamiltonian:

$$H = \sum_{k,\sigma} \psi_k^{\sigma,+} H_k \psi_k^{\sigma,-} + \frac{1}{2} \sum_k \sum_{\alpha,\beta=1}^2 \rho_k^\alpha V_{\alpha\beta}(k) \rho_{-k}^\beta. \quad (2.1)$$

Here $\psi_k^\sigma = (a_1^\sigma(k), b_1^\sigma(k), a_2^\sigma(k), b_2^\sigma(k))^T$, and $a^{\alpha\sigma}(k)$ and $b^{\alpha\sigma}(k)$ are destruction operators of the Bloch states of the two triangular sublattices on the graphene layers $\alpha = 1, 2$ with the additional flavor index σ that encodes spin and valley. Further, ρ_q^α is the electron density on layer α , $V_{11}(k) = V_{22}(k) = 2\pi e^2 / (\kappa k)$ is the Coulomb interaction of electrons on the same layer, and electrons on different layers interact via $V_{12}(k) = V_{21}(k) = V_{11}(k)e^{-kd}$, where d is the distance between the layers and κ is the dielectric permittivity of the substrate. The one-particle Hamiltonian has the following form:

$$H_k = \begin{pmatrix} 0 & \xi \epsilon(k) & 0 & t_\perp \\ \xi \epsilon^*(k) & 0 & 0 & 0 \\ 0 & 0 & 0 & \xi \epsilon(k) \\ t_\perp & 0 & \xi \epsilon^*(k) & 0 \end{pmatrix}, \quad (2.2)$$

where $t_\perp \sim 0.4 \text{ eV}$ is the interlayer hopping amplitude, $\epsilon(k) = \hbar v_F (k_x + ik_y)$, and the vector $\mathbf{k} = (k_x, k_y)$ describes a deviation from the K ($\xi = 1$) and K' ($\xi = -1$) points in the Brillouin zone.²⁴ Below we will consider only the K valley. The one-particle Hamiltonian can be diagonalized with the help of the unitary matrix U . Then one obtains the following four-band spectrum:

$$H_k = U_k^{-1} \text{diag}(E_k^+, -E_k^+, E_k^-, -E_k^-) U_k, \quad (2.3)$$

$$E_q^\pm = \sqrt{(\hbar v_F k)^2 + t_\perp^2/4} \pm t_\perp/2. \quad (2.4)$$

In what follows, for simplicity we set $t_\perp = t$ and rescale all momenta by $k \rightarrow k/\hbar v_F$. Then the Fermi momentum equals

$k_F = \sqrt{\mu(\mu + t)}$ and the charge density at zero temperature is given by $n \approx k_F^2/t^2 \times 10^{13} \text{ cm}^{-2}$. The charge density $n = 10^{12} \text{ cm}^{-2}$ corresponds to $\mu/t = 0.1$, while the higher density $n = 10^{13} \text{ cm}^{-2}$ corresponds to $k_F = t$ and $\mu/t \approx 0.6$. Here μ is the chemical potential (Fermi energy). In the usual units, $k_F = t$ corresponds to $k_F \approx 0.06 \text{ \AA}^{-1}$.

If we denote the polarization matrix as $-i\langle \rho_\alpha(\omega, \mathbf{k}) \rho_\beta(-\omega, \mathbf{k}) \rangle = \delta^{(3)}(k - \tilde{k}) 2\Pi_{\alpha\beta}(k)$, then the interaction potential in the RPA is given by

$$V_{11}^{\text{eff}}(k) = \frac{k - \alpha(1 - e^{-2kd})\Pi_{11}}{k\epsilon(\omega, k)[k - \alpha(1 - e^{-kd})(\Pi_{11} - \Pi_{12})]}, \quad (2.5)$$

$$V_{12}^{\text{eff}}(k) = \frac{ke^{-kd} + \alpha(1 - e^{-2kd})\Pi_{12}}{k\epsilon(\omega, k)[k - \alpha(1 - e^{-kd})(\Pi_{11} - \Pi_{12})]}, \quad (2.6)$$

$$\epsilon(\omega, k) = 1 - \frac{\alpha(1 + e^{-kd})}{k}(\Pi_{11} + \Pi_{12}). \quad (2.7)$$

Here $\alpha = e^2/(\hbar v_F \kappa)$ is the effective coupling constant in graphene and $d \approx 3 \text{ \AA}$ is the distance between the graphene layers, which is relatively small, so in all exponents we can set $d = 0$ (even for the largest possible momentum $e^{-k_F d} \approx 0.85$). Then we have $V_{11}^{\text{eff}} = V_{12}^{\text{eff}} = 1/k\epsilon(\omega, k)$, where the dielectric permittivity equals $\epsilon(\omega, k) = 1 - \alpha\Pi(\omega, k)/k$ with $\Pi \equiv 2(\Pi_{11} + \Pi_{12})$. The system is degenerate with respect to spin and valley degrees of freedom; therefore now we will consider polarization for one flavor degree of freedom: $\Pi \rightarrow \Pi/N_f$, $N_f = 4$. Then the one-loop polarization is given by

$$\Pi(\omega, k) = T \sum_{n=-\infty}^{\infty} \int \frac{d^2q}{2\pi} \text{Tr} G(i\Omega_n, q) G(i\Omega_n + i\omega_m, q + k). \quad (2.8)$$

Summation over the Matsubara frequency can easily be done.²⁸ Then, performing the analytic continuation through the replacement $i\omega_m \rightarrow \omega + i0$, we obtain the retarded polarization function as

$$\begin{aligned} \Pi(\omega, k) &= \int \frac{d^2q}{2\pi} \sum_{\alpha, \alpha'=\pm 1} \sum_{\lambda, \lambda'=1, 2} \\ &\times \frac{n_F[(-1)^\lambda E_q^\alpha] - n_F[(-1)^{\lambda'} E_{q+k}^{\alpha'}]}{(-1)^\lambda E_q^\alpha - (-1)^{\lambda'} E_{q+k}^{\alpha'} - \omega - i0} \\ &\times F_{\lambda+1-\alpha, \lambda'+1-\alpha'}(q, q+k), \end{aligned} \quad (2.9)$$

where the indices λ and α denote bands and F_{ij} is a 4×4 matrix responsible for the chiral structure. It is defined as follows:

$$F_{ij}(q, p) = \text{Tr}(Z^{-1} \Delta_i Z \Delta_j), \quad Z = U_q^{-1} U_p, \quad (2.10)$$

and Δ_j is a diagonal matrix with all zero elements except for unity at position j . We find

$$F(q, p) = \begin{pmatrix} U^{++} & V^{--} & V^{+-} & U^{+-} \\ V^{--} & U^{++} & U^{+-} & V^{+-} \\ V^{+-} & U^{+-} & U^{--} & V^{++} \\ U^{+-} & V^{+-} & V^{++} & U^{--} \end{pmatrix}, \quad (2.11)$$

where

$$U^{su} = \frac{E_q^{(s)} E_p^{(u)}}{4E_q^{(0)} E_p^{(0)}} \left(1 + su \frac{qp \cos \theta_{qp}}{E_q^{(s)} E_p^{(u)}} \right)^2, \quad (2.12)$$

$$V^{su} = \frac{E_q^{(s)} E_p^{(u)}}{4E_q^{(0)} E_p^{(0)}} \sin^2 \theta_{qp}, \quad (2.13)$$

$E_q^{(s)} = \sqrt{q^2 + t^2/4} + st/2$, and θ_{qp} is the angle between vectors \mathbf{p} and \mathbf{q} . Diagonal elements of F describe intraband transitions while off-diagonal elements are responsible for interband ones. At zero temperature, the Fermi functions in Eq. (2.9) reduce to simple step functions. Then our retarded polarization can be presented in the following form:

$$\Pi(\omega, k) = \Pi^0(\omega, k) + \Pi^+(\omega, k) + \Pi^-(\omega, k), \quad (2.14)$$

where

$$\begin{aligned} \Pi^0(\omega, k) &= \int \frac{d^2q}{\pi} \sum_{s=\pm} \left(\frac{E_{q+k}^{(s)} + E_q^{(-s)}}{\omega^2 - (E_{q+k}^{(s)} + E_q^{(-s)})^2} U^{-s, s} \right. \\ &\left. + \frac{E_{q+k}^{(-s)} + E_q^{(s)}}{\omega^2 - (E_{q+k}^{(-s)} + E_q^{(s)})^2} V^{s, s} \right), \end{aligned} \quad (2.15)$$

$$\begin{aligned} \Pi^u(\omega, k) &= \int_{E_q^{(u)} < \mu} \frac{d^2q}{\pi} \sum_{s=\pm} \left(\frac{us E_{q+k}^{(s)} - E_q^{(u)}}{\omega^2 - (us E_{q+k}^{(s)} - E_q^{(u)})^2} U^{u, s} \right. \\ &\left. + \frac{us E_{q+k}^{(-s)} - E_q^{(u)}}{\omega^2 - (us E_{q+k}^{(-s)} - E_q^{(u)})^2} V^{-u, s} \right), \quad u = \pm. \end{aligned} \quad (2.16)$$

Clearly, Π^0 does not depend on the chemical potential and characterizes the polarization at zero doping. It gives the main contribution to screening. The functions Π^+ and Π^- incorporate the effects of doping and are mainly responsible for plasmon modes. It is obvious that Π^+ can be evaluated immediately if Π^- is found for arbitrary values of μ and t . We have $\Pi_{\mu, t}^+ = \theta(\mu - t) \Pi_{\mu-t, -t}^-$.

Let us comment on the chirality matrix (2.11). In the two limiting cases of weak ($t \rightarrow 0$) and strong ($t \rightarrow \infty$) coupling, when the spectrum reduces to $E_q = q$ and $E_q = q^2/t$, respectively, the chirality matrix F is greatly simplified and depends only on one parameter u_q . Then the polarization function per one flavor degree of freedom²⁹ equals

$$\begin{aligned} \Pi(\omega, k) &= \int_{E_q > \mu} \frac{d^2q}{\pi} \frac{1 - u_{q, k}}{2} \frac{E_q + E_{q+k}}{\omega^2 - (E_q + E_{q+k})^2} \\ &+ \int_{E_q < \mu} \frac{d^2q}{\pi} \frac{1 + u_{q, k}}{2} \frac{E_{q+k} - E_q}{\omega^2 - (E_q - E_{q+k})^2}, \end{aligned} \quad (2.17)$$

where $u_{q, k} = (\text{Tr} H_q H_{q+k}) / (2E_q E_{q+k})$, which is equal to $\cos \theta_{q, q+k}$ and $\cos 2\theta_{q, q+k}$ for weak and strong coupling, respectively. Note that at weak coupling $\Pi^+ = \Pi^-$ while $\Pi^+ = 0$ at strong coupling.

In what follows we will consider an intermediate case for which $\mu < t$ (only this regime is experimentally relevant). In this case, $\Pi^+ = 0$. Calculation of Π^0 and Π^- is straightforward and the result can be written down in the following

compact form:

$$\Pi(\omega, k) = \Pi^0(\omega, k) + \Pi^-(\omega, k) = -\frac{2\mu + t}{2} - \frac{k^2 t}{4(k^2 - \omega^2)} + \frac{P_\omega + \overline{P}_\omega}{4} - c_\omega \overline{g}_\omega + \overline{g}_{t-\omega} + \overline{g}_{t+\omega}, \quad (2.18)$$

where

$$P_\omega = G_{\omega+t} - c_\omega G_\omega + i \frac{\mu_\star}{2} \sqrt{\frac{\rho_\omega^2 - \mu_\star^2}{\omega^2 - k^2} + i0} \frac{k^2 + \omega \mu_\star}{\omega^2 - k^2} + \frac{k^2 - \omega(t + \omega)}{2\omega} \ln \frac{\rho_\omega^{-2} k^4 \mu^2}{|(k^2 - \omega^2)[k^2 - \omega(2t + \omega)]|} \\ + \frac{Q_{-\omega}^{\mu_\star} - Q_{+,-\omega-t}^{\omega-2\mu} + Q_{-,-\omega-t}^{2\mu-\omega} - Q_{-,-\omega}^{\mu_\star}}{2\omega} - \frac{i\pi |k^2 - \omega(t + \omega)|}{2\omega} \{\theta[\omega^2 - k^2 - t^2] - \theta[\omega(\omega + 2t) - k^2]\} \quad (2.19)$$

with

$$c_\omega = \frac{3k^4 - k^2(t^2 + 5\omega^2) + 2\omega^4}{2(\omega^2 - k^2)^2}, \quad \rho_\omega = k \sqrt{\frac{\omega^2 - k^2 - t^2}{\omega^2 - k^2}}, \quad \mu_\star = 2\mu + t - \omega, \quad g_\omega = \frac{\sqrt{k^2 - \omega^2}}{2} \tan^{-1} \frac{\sqrt{k^2 - \omega^2}}{t}, \quad (2.20)$$

$$G_\omega = \sqrt{\omega^2 - k^2} \left[\ln \left(\mu_\star \operatorname{sgn}(k^2 - \omega^2) + \sqrt{k^2 - \omega^2} \sqrt{\frac{\rho_\omega^2 - \mu_\star^2}{\omega^2 - k^2} + i0} \frac{k^2 + \omega \mu_\star}{\omega^2 - k^2} \right) + (\mu_\star \rightarrow t - \omega) \right], \quad (2.21)$$

$$Q_{\pm, \omega}^r = |k^2 - \omega(t + \omega)| \ln \left(y + i \sqrt{\operatorname{sgn} \rho_\omega^2 - y^2 + i0} \frac{k^2 \pm \omega r}{\omega^2 - k^2} \right), \quad y = \frac{\rho_\omega^2 - r(\omega + t)}{|\rho_\omega(r - \omega - t)|}. \quad (2.22)$$

Here the expressions $i0(\dots)$ are responsible for choosing the correct branch of the cuts. The square root and logarithm have a branch cut discontinuity in the complex plane running from $-\infty$ to 0. Equations (2.18)–(2.22) are our main results. Details of the calculations as well as the expressions for the real and imaginary parts are given in Appendixes 1 and 2. In the weak-coupling limit $t \rightarrow 0$, one can easily reproduce the results obtained in Ref. 15 up to the overall factor 2 which reflects the bilayer nature of the system [in this case we should formally assume that $\mu > t$ and take into account $\Pi^+(\omega, k)$]. In the strong-coupling limit $t \gg \mu, k, \omega$, in order to reproduce the results obtained in Ref. 17 one should take into account terms of order $E_k = k^2/t$.

It is convenient to normalize the polarization with respect to the density of states at the Fermi level, $D(\mu) = N_f(t + 2\mu)/4\pi$. So we introduce the normalized polarization

$$\hat{\Pi}(\omega, k) \equiv -2 \frac{\Pi^0(\omega, k) + \Pi^-(\omega, k)}{t + 2\mu}. \quad (2.23)$$

Finally, the dielectric permittivity in terms of the normalized polarization is given by

$$\epsilon(\omega, k) = \kappa \left(1 + 2\pi\alpha D(\mu) \frac{\hat{\Pi}(\omega, k)}{k} \right), \quad \alpha = \frac{e^2}{\hbar v_F \kappa}. \quad (2.24)$$

In Fig. 1 we plot $\hat{\Pi}(\omega, k)$ for $\mu/t = 0.6$. Note that the corresponding plots are very similar to those in Ref. 3. The static case $\omega = 0$ and the long-wavelength limit $k \rightarrow 0$ are considered in Secs. III A and III B.

III. ANALYSIS OF TWO PARTICULAR CASES

A. Static screening

The static limit $\omega \rightarrow 0$ is relevant for screening of charged impurities. Performing some mathematical transformations, we find that Eqs. (2.18)–(2.22) imply

$$\Pi(\omega = 0, k) = \frac{t}{2} \ln \frac{\sqrt{k^2 + t^2}}{\mu} - \frac{t}{4} - \mu - \frac{3k^2 - t^2}{4k} \\ \times \tan^{-1} \frac{k}{t} - \sqrt{t^2 - k^2} \tanh^{-1} \frac{\sqrt{t^2 - k^2}}{t} \\ + \left[\sqrt{k^2 - 4\mu(t + \mu)} \left(\frac{t + 2\mu}{2k} + \frac{k}{2\mu} \right) - \frac{3k^2 - t^2}{2k} \cos^{-1} \frac{t + 2\mu}{\sqrt{k^2 + t^2}} - t \tanh^{-1} \frac{k\sqrt{k^2 - 4\mu(t + \mu)}}{k^2 - 2t\mu} \right] \\ \times \frac{\theta[k^2 - 4\mu(t + \mu)]}{2} + \left(\sqrt{t^2 - k^2} \sinh^{-1} \right. \\ \left. \times \frac{2\mu\sqrt{t^2 - k^2}}{k^2} - \sqrt{\frac{k^4}{4\mu^2} - k^2 + t^2} \right) \\ \times \frac{\theta[k^4 - 4k^2\mu^2 + 4t^2\mu^2]}{2}. \quad (3.1)$$

The behavior of the normalized static polarization $\Pi(k) \equiv -2\hat{\Pi}(\omega = 0, k)/(t + 2\mu)$ and the corresponding polarizations for monolayer¹⁵ and bilayer graphene in the two-band approximation¹⁷ are shown in Figs. 2(a)–2(c) as functions of the normalized momentum k/k_F . We see that the polarization function calculated in the four-band model has a discontinuity at $k = 2k_F$ similar to that found in the two-band model

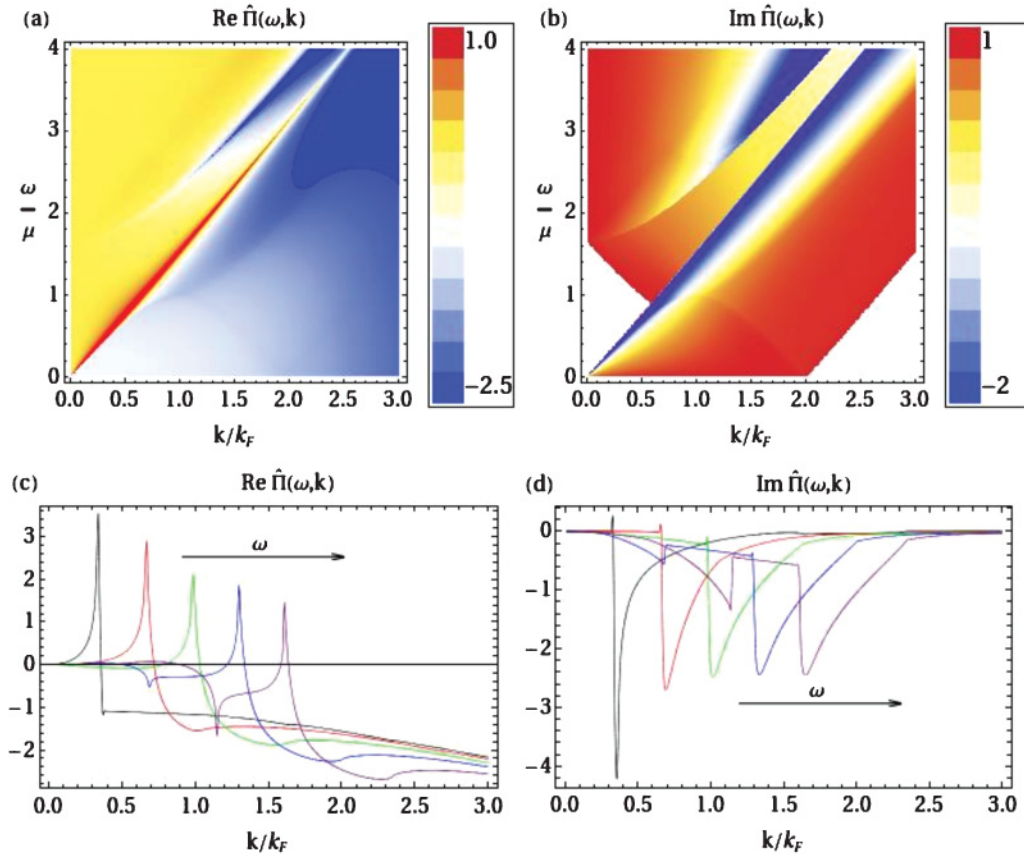


FIG. 1. (Color online) Normalized polarization function for $\mu/t = 0.6$. (a) and (b) show density plots of the real and imaginary parts of the normalized polarization bubble defined in Eq. (2.18), respectively. (c) and (d) present constant-frequency cuts for $\omega/\mu = 0.5, 1.0, 1.5, 2.0, 2.5$.

[see Fig. 2(e)]; however, it does not go to a constant value at large momenta. Rather, it grows linearly as in the case of monolayer graphene [see Fig. 2(f)]. For $\mu/t \rightarrow 0$, the polarization function is similar to the polarization function in the two-band model¹⁷ and tends to the SLG polarization function for $\mu/t \gg 1$. The dielectric permittivity at large k for bilayer graphene in the four-band model equals $\epsilon(k) = 1 + \pi\alpha N_f/4$, whereas $\epsilon(k) = 1$ in the two-band model. Note that $\epsilon(k) = 1 + \pi\alpha N_f/8$ for the SLG; therefore, we conclude that permittivities in the BLG in the four-band model and the SLG coincide in view of the replacement $N_f \rightarrow 2N_f$ for the BLG due to doubling of the number of layers.

Since the static polarization depends only on the absolute value of the momentum, the RPA improved Coulomb potential is given by the following formula:

$$V(r) = \int_0^\infty dk \frac{k J_0(kr)}{k + 2\pi\alpha D(\mu)\Pi(k)}. \quad (3.2)$$

At finite doping the polarization function has a discontinuity at $k = 2k_F$; therefore, at large distances the potential behaves as

$$V(r) \sim \frac{1}{r} \frac{\sin(rk_F)}{rk_F}, \quad rk_F \rightarrow \infty. \quad (3.3)$$

For zero doping, the discontinuity is absent and the leading asymptote is determined by the long-wavelength behavior of the polarization function. We find

$$V(r) \sim \frac{1}{r} \frac{1}{(rt)^2}, \quad rt \rightarrow \infty. \quad (3.4)$$

The RPA improved Coulomb potential is shown in Fig. 3.

B. Plasmons

The polarization function in the long-wavelength limit $k \ll t$ is given by the following expression:

$$\begin{aligned} \Pi(\omega, k) = & \frac{k^2}{2\omega^2} \left(\mu + t + \frac{t^2}{4\omega} \ln \frac{2\mu + t - \omega}{2\mu + t + \omega} \right. \\ & + \frac{t^2}{4\omega} \ln \frac{\omega - t}{t + \omega} + \frac{\omega(\omega + 2t)}{4(t + \omega)} \ln \frac{2\mu - \omega}{2t + \omega} \\ & \left. - \frac{\omega(\omega - 2t)}{4(t - \omega)} \ln \frac{2t - \omega}{2\mu + \omega} \right). \end{aligned} \quad (3.5)$$

If ω is small then

$$\Pi(\omega, k) = \frac{k^2\mu(\mu + t)}{\omega^2(t + 2\mu)}. \quad (3.6)$$

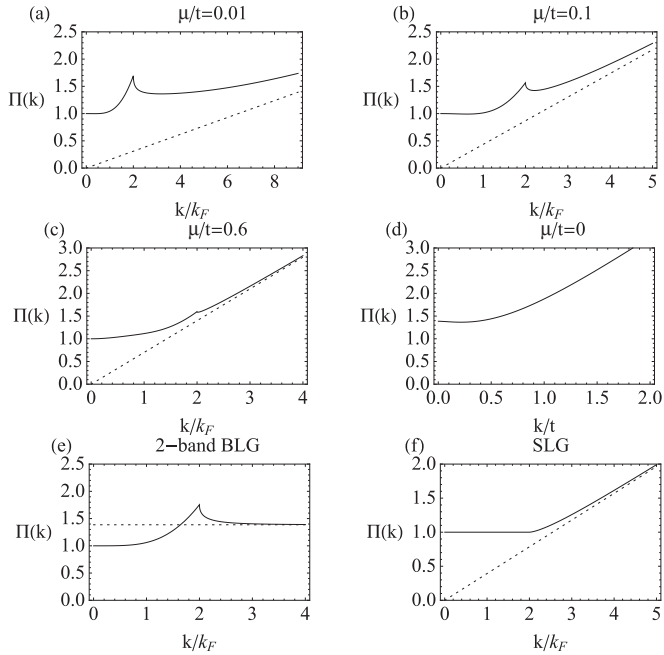


FIG. 2. The static polarization. (a), (b), and (c) show plots of the normalized static polarization given by (3.1) at $\mu/t = 0.01, 0.1$, and 0.6 , respectively. Dotted lines correspond to the asymptotic values $\Pi(k) = \pi k/2(t + 2\mu)$. In (e) and (f) we show, respectively, the static limit of the polarization function for the bilayer graphene in the two-band approximation obtained in Ref. 17 and monolayer graphene calculated in the Dirac approximation in Refs. 15, 25, and 3. The dotted line in (e) corresponds to the asymptotic value $\Pi(k) = \ln 4$ while the asymptote in (f) is $\Pi(k) = \pi k/8\mu$.

The plasmon dispersion relation is determined by the equation $\epsilon(k, \omega(k)) = 0$ which immediately gives

$$\omega(k) = \sqrt{k \frac{e^2 N_f}{\kappa} \frac{\mu(\mu + t)}{\mu + 2t}}. \quad (3.7)$$

This is the general expression for the plasmon mode in two-dimensional (2D) systems, which for the general spectrum of quasiparticle excitations can be written as¹⁷

$$\omega(k) = \sqrt{k \frac{e^2 N_f}{2\kappa} q \left. \frac{\partial E_q}{\partial q} \right|_{q=q_F}}. \quad (3.8)$$

Equivalently, this formula can be written as

$$\omega(k) = 2\pi \sqrt{k \frac{e^2 N_f}{\kappa} \frac{n}{D(\mu)}}, \quad (3.9)$$

where $n = N_f k_F^2/4\pi$ is the actual two-dimensional density of particles while $D(\mu)$ is the density of states at the Fermi level. In the case of the SLG $D(\mu) \sim \sqrt{n}$ so $\omega(k) \sim k^{1/2} n^{1/4}$.

We solved the equation $\text{Re}[\epsilon(k, \omega(k))] = 0$ numerically for free-standing graphene (i.e., $\kappa = 1$). Results are shown at Fig. 4. We see that except for ‘‘classical’’ plasmons with the low-energy behavior (3.8), we also have modes with linear behavior and high-energy modes that are analogous to the π

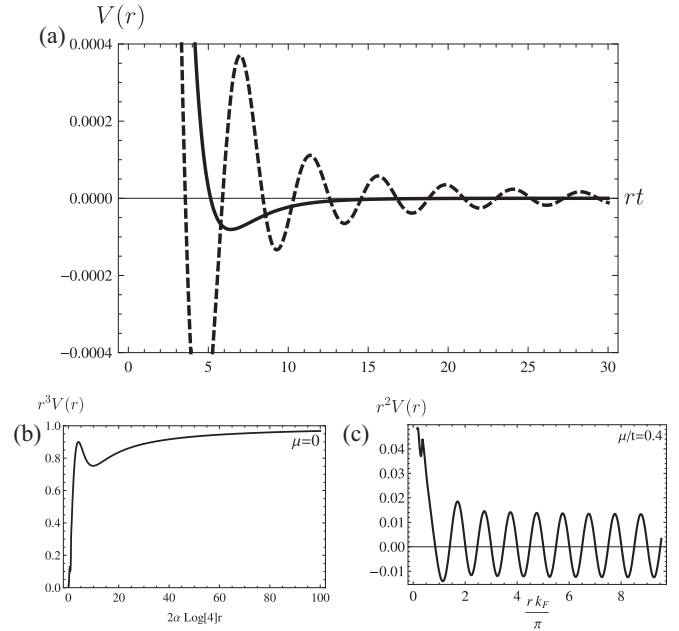


FIG. 3. The RPA improved Coulomb potential at finite and zero doping. In (a) the dashed line corresponds to the potential at $\mu = 0.4t$ and the solid line to zero μ . (b) and (c) show asymptotes of the RPA improved potential at zero and finite doping, respectively.

plasmons.²⁶ The corresponding dispersion relation for small momenta are

$$\omega(k) = \frac{2k(t + \mu)}{t + 2\mu} - \frac{k^2 t^2 \mu(t + \mu)^2}{(t + 2\mu)^3}, \quad (3.10)$$

$$\omega(k) = t + \frac{e^2 N_f}{2\kappa} k \ln \left(1 + \frac{2\mu}{t} \right). \quad (3.11)$$

However, in contrast to the classical plasmons these modes cannot be considered as fully coherent collective modes, because they lie in the highly damped area which corresponds to the gray shading on the plots. The boundaries of the damped area are determined by the equation $\text{Im}\Pi(k, \omega(k)) = 0$ which can be easily solved, and we obtain

$$\omega_{\pm}(k) = \sqrt{\frac{t^2}{4} + (k \pm k_F)^2} - \left| \frac{t}{2} \pm \mu \right|, \quad (3.12)$$

which describes the boundary of the single-particle excitation continuum (Landau damping). Note that, in contrast to the normal 2D electron gas, plasmons are damped at smaller momenta due to the interband transitions.

All the described plasmons vanish at zero chemical potential, which is consistent with the classical picture where plasma oscillations are absent without matter. However, in the quantum case this directly follows from the form of the elementary excitation spectrum. Taking into account the effects of ‘‘trigonal warping,’’ the low-energy spectrum transforms into⁵

$$E_{\mathbf{k}} = \frac{\hbar^2 v_F^2 k^2}{t} \rightarrow \frac{\hbar^2 v_F^2 k \sqrt{k^2 + k_0^2 - 2kk_0 \cos 3\phi}}{t}, \quad (3.13)$$

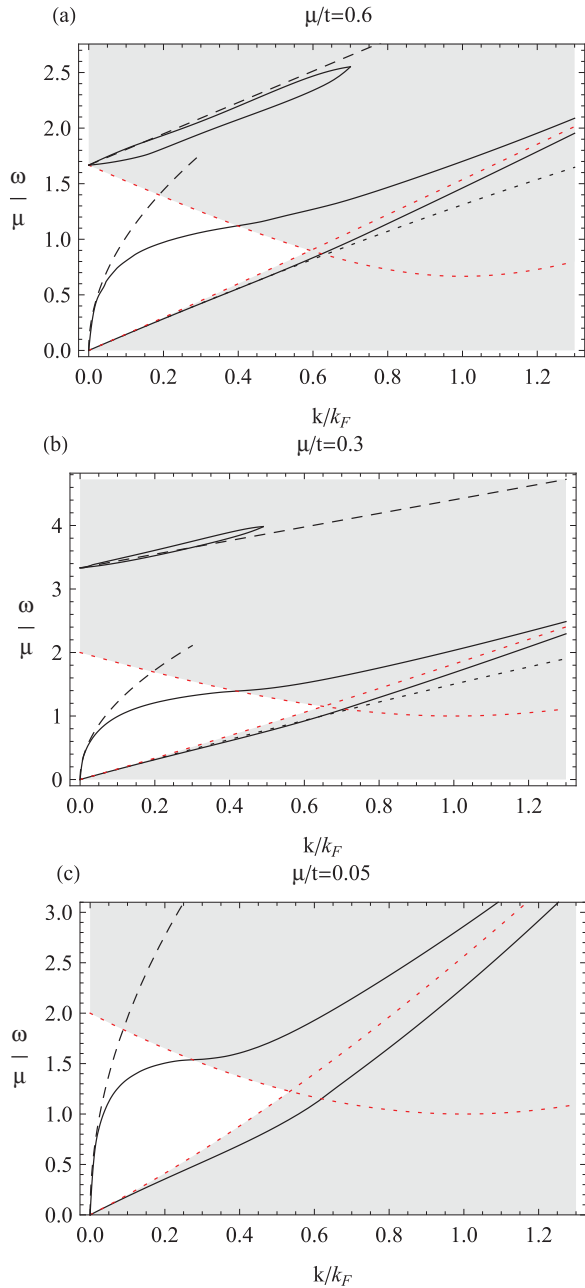


FIG. 4. (Color online) (a), (b), and (c) present the dispersion relations (black solid lines) for plasmons in free-standing graphene at densities $\mu/t = 0.6, 0.3,$ and 0.05 respectively. Black dashed lines describe the classical plasmon (3.8) and the high-energy plasmon (3.11). Black dotted lines describe the additional low-energy plasmon given by (3.10). Filled areas show domains with nonzero imaginary part of the polarization whose boundaries (red dotted lines) are given by Eqs. (3.12).

where $k_0 \approx 5.7 \times 10^7 \text{ m}^{-1}$. In this case, as was shown in Ref. 27, there exist weakly damped plasmons. The approximate form of the dispersion relation can be estimated as

$$\omega \approx E_0 \sqrt{\frac{N_f e^2}{\hbar v_0} \frac{k}{k_0}} \approx 12.5 E_0 \sqrt{\frac{k}{k_0}}, \quad (3.14)$$

where $E_0 = \hbar^2 v_f^2 k_0^2 / t \approx 3.9 \text{ meV}$ and $v_0 = E_0 / (\hbar k_0) = 10^5 \text{ m/s}$. As one can see these plasmons disappear for $k_0 \rightarrow 0$.

IV. CONCLUSION

In this paper we have derived a compact analytic expression for the dynamical polarization for bilayer graphene in the four-band model in the random phase approximation. Our results are valid for arbitrary values of the wave vector, frequency, doping, and interlayer coupling. Analyzing the polarization as a function of the interlayer coupling, we recovered the expressions for monolayer graphene polarization (weak coupling) as well as for bilayer graphene in the two-band model (strong coupling). In the case where the doping is smaller than the interlayer coupling we found the polarization function in the static and long-wavelength limits. Using these results, we obtained the RPA improved Coulomb interaction and the dispersion relation for the plasmon mode.

We put aside temperature effects and effects of the finite distance between layers; however, within this formalism they can be easily investigated and we postpone this investigation for a separate presentation.

ACKNOWLEDGMENTS

The author is grateful to Yu. V. Bezvershenko, V. P. Gusynin, E. V. Gorbar, A. B. Kashuba, and Y. F. Suprunenko for valuable discussions and useful remarks. The author is especially grateful to Artur Slobodeniuk for collaboration in the initial stage of the work. The work was supported partially by the SCOPES Grant No. IZ73Z0 128026 of the Swiss NSF, by the grant SIMTECH No. 246937 of the European FP7 program, and by SFFR-RFBR Grant ‘‘Application of string theory and field theory methods to nonlinear phenomena in low dimensional systems.’’

APPENDIX: CALCULATION OF THE POLARIZATION FUNCTION

In this Appendix we present some major steps in the calculation of the normalized polarization function. All quantities are evaluated in units of energy (Sec. II). We restrict our consideration to the case $\omega > 0$ because the polarization function for negative ω can be obtained through complex conjugation.

1. $\Pi^0(\omega, k)$ calculation

In order to calculate $\Pi^0(\omega, k)$ given by (2.15), it is convenient to introduce the following variables:

$$y = E_q + E_{q+k}, \quad z = 4E_q E_{q+k}. \quad (A1)$$

Then the measure of integration transforms as follows:

$$\begin{aligned} \int q dq d\theta &= 2 \int dq^2 \int_0^{\pi/2} d\theta \\ &= \frac{1}{2} \int_{\sqrt{k^2+i^2}}^y \frac{dy}{\sqrt{y^2-k^2}} \int_Q^{y^2} \frac{z dz}{\sqrt{y^2-z}\sqrt{z-Q}}, \end{aligned} \quad (A2)$$

$$Q = \frac{(y^2 - k^2)^2 + t^2 k^2}{y^2 - k^2}. \quad (\text{A3})$$

Performing integration over z , we get

$$\Pi^0(\omega, k) = \int_{\sqrt{k^2+t^2}}^y \frac{dy}{2} \left(\frac{\sqrt{y^2 - k^2}(y - t)}{\omega^2 - (y - t)^2} + \frac{\sqrt{y^2 - k^2}(t + y)}{\omega^2 - (t + y)^2} - \frac{y[3k^4 - k^2(t^2 + 5y^2) + 2y^4]}{(y^2 - k^2)^{3/2}(\omega^2 - y^2)} \right) + \delta\Pi^0(\omega, k), \quad (\text{A4})$$

where $\delta\Pi^0(\omega, k)$ is obtained by the proper change of variables,

$$\delta\Pi^0(\omega, k) = \left(\int_{\sqrt{t^2+k^2}}^{\sqrt{t^2/4+k^2}-t/2} + \int_{\sqrt{t^2+k^2}-t}^{\sqrt{t^2/4+k^2}-t/2} - \int_{-t/2-\sqrt{t^2+k^2}}^{-\sqrt{t^2+k^2}-t} - \int_{-t/2-\sqrt{t^2/4+k^2}}^{-\sqrt{t^2+k^2}} \right) \frac{dy}{2} \frac{\omega^2 + yt - k^2}{\omega^2 - y^2}. \quad (\text{A5})$$

Now we can easily calculate the imaginary part for $\omega > 0$:

$$\begin{aligned} \frac{\text{Im}\Pi^0(\omega, k)}{\pi} &= \left(\frac{3k^4 - k^2(t^2 + 5\omega^2) + 2\omega^4}{4(\omega^2 - k^2)^{3/2}} - \frac{|k^2 - \omega(\omega - t)| + |k^2 - \omega(\omega + t)|}{4\omega} \right) \theta(\omega - \sqrt{t^2 + k^2}) \\ &+ \theta(\omega + t - \sqrt{t^2 + k^2}) \left(\frac{|k^2 - \omega(\omega + t)|}{4\omega} - \frac{\sqrt{(\omega + t)^2 - k^2}}{4} \right) \\ &+ \theta(\omega - t - \sqrt{t^2 + k^2}) \left(\frac{|k^2 - \omega(\omega - t)|}{4\omega} - \frac{\sqrt{(\omega - t)^2 - k^2}}{4} \right). \end{aligned} \quad (\text{A6})$$

The real part is calculated treating all divergences in the principal value sense. After some algebra we obtain

$$\begin{aligned} \text{Re}\Pi^0(\omega, k) &= \frac{k^2 t}{2(\omega^2 - k^2)} - \text{Re} \left[\frac{3k^4 - k^2(t^2 + 5\omega^2) + 2\omega^4}{2(k^2 - \omega^2)^{3/2}} \tan^{-1} \frac{\sqrt{k^2 - \omega^2}}{t} \right] \\ &+ \frac{[k^2 - \omega(\omega - t)]}{4\omega} \ln \left| \frac{[k^2 + (2t - \omega)\omega](k^2 + t^2 - \omega^2)}{(k^2 + (t - \omega)\omega)^2} \right| - \frac{k^2 - \omega(t + \omega)}{4\omega} \ln \left| \frac{(k^2 + t^2 - \omega^2)[k^2 - \omega(2t + \omega)]}{[k^2 - \omega(t + \omega)]^2} \right| \\ &+ \text{Re} \left[\frac{\sqrt{k^2 - (t - \omega)^2}}{2} \tan^{-1} \left(\frac{\sqrt{k^2 - (t - \omega)^2}}{t} \right) + \frac{\sqrt{k^2 - (t + \omega)^2}}{2} \tan^{-1} \left(\frac{\sqrt{k^2 - (t + \omega)^2}}{t} \right) \right]. \end{aligned} \quad (\text{A7})$$

In the $t \rightarrow 0$ limit, we get

$$\lim_{t \rightarrow 0} \Pi^0(\omega, k) = -\frac{\pi}{4} \frac{k^2}{\sqrt{k^2 - \omega^2 - i0}}, \quad (\text{A8})$$

where we performed the shift $\omega^2 \rightarrow \omega^2 + i0$ in order to reproduce the correct imaginary part.

In the large- t limit we must retain terms of order $k^2/t = E_k$. Then t appears only as an overall factor:

$$\frac{\Pi^0(\omega, k)}{t/2} = \ln \left| \frac{E_k^2 - 4\omega^2}{4E_k^2 - 4\omega^2} \right| + \frac{E_k}{2\omega} \ln \left| \frac{(E_k - \omega)^2 E_k + 2\omega}{(E_k + \omega)^2 E_k - 2\omega} \right| + i\pi \left[\left(1 - \frac{E_k}{\omega}\right) \theta[\omega - E_k] - \left(1 - \frac{E_k}{2\omega}\right) \theta[2\omega - E_k] \right]. \quad (\text{A9})$$

2. $\Pi^-(\omega, k)$ calculation

In order to calculate $\Pi^-(\omega, k)$ given by (2.16) we introduce the new variable $r = E_q - t/2$. Then, performing some algebraic manipulations, we find

$$\Pi^-(\omega, k) = \int_0^\mu \frac{dr}{r} \int_0^{2\pi} \frac{d\phi}{16\pi} \left(\frac{g(\omega)}{r+\omega} + \frac{g(-\omega)}{r-\omega} - 8r - 4t \right), \quad (\text{A10})$$

where

$$g(\omega) = \frac{k^4 - 2k^2[2r^2 + 2r\omega + \omega(\omega - t)] + (2r + \omega)^2(t - \omega)^2}{k^2 + 2k\sqrt{r(r+t)}\cos\phi + (2r + \omega)(t - \omega)} - \frac{[k^2 - (2r + \omega)(2r + t + \omega)]^2}{k^2 + 2k\sqrt{r(r+t)}\cos\phi - \omega(2r + t + \omega)}. \quad (\text{A11})$$

All divergences should be dealt with using the prescription $\omega \rightarrow \omega + i0$. Then we can integrate over the angle using the following integral:

$$\frac{1}{2\pi} \int_0^{2\pi} \frac{d\phi}{a + i\epsilon 0 + \cos\phi} = \frac{\text{sgn}[a]\theta(a^2 - 1)}{\sqrt{a^2 - 1}} - i \frac{\text{sgn}[\epsilon]\theta(1 - a^2)}{\sqrt{1 - a^2}}. \quad (\text{A12})$$

We obtain the real and imaginary parts of the polarization function:

$$\begin{aligned} \text{Re}\Pi^-(\omega, k) &= \int_0^\mu \frac{dr}{2r} \left(\frac{\text{Re}[g_R(\omega)]}{4(r + \omega)} \right. \\ &\quad \left. + \frac{\text{Re}[g_R(-\omega)]}{4(r - \omega)} - 2r - t \right), \quad \text{Im}\Pi^-(\omega, k) \\ &= - \int_0^\mu \frac{dr}{8r} \left(\frac{\text{Re}[g_I(\omega)]}{r + \omega} - \frac{\text{Re}[g_I(-\omega)]}{r - \omega} \right), \end{aligned} \quad (\text{A13})$$

$$g_R(\omega) = \frac{\sqrt{[k^2 + (2r + \omega)(t - \omega)]^2 - 4k^2r(r + t)}\text{sgn}[k^2 + (2r + \omega)(t - \omega)] - [k^2 - (2r + \omega)(2r + t + \omega)]^2\text{sgn}[k^2 - \omega(2r + t + \omega)]}{\sqrt{[k^2 - \omega(2r + t + \omega)]^2 - 4k^2r(r + t)}}, \quad (\text{A14})$$

$$g_I(\omega) = \frac{\sqrt{4k^2r(r + t) - [k^2 + (2r + \omega)(t - \omega)]^2}\text{sgn}\left(r - \frac{t}{2} + \omega\right) + \frac{[k^2 - (2r + \omega)(2r + t + \omega)]^2\text{sgn}\left(r + \frac{t}{2} + \omega\right)}{\sqrt{4k^2r(r + t) - [k^2 - \omega(2r + t + \omega)]^2}}}{}. \quad (\text{A15})$$

We can calculate all the integrals separately keeping the regularization ϵ of possible divergences at $r = 0$. In order to write down the answer in a compact form, we introduce the following notation. For any given function $f(x)$, one can construct a new function $\widehat{f}(x)|_a^b$ by the following rule:³⁰

$$\widehat{f}(x)|_a^b \equiv \text{sgn}(b - x)[f(b) - f(x)] - \text{sgn}(a - x)[f(a) - f(x)]. \quad (\text{A16})$$

Then one can present the polarization in the following form:

$$\Pi_\epsilon^-(\omega, k) = -\mu - \frac{t}{2} \ln \frac{2\mu}{\epsilon} + \frac{\text{Re}(R_\omega + R_{-\omega}) + i\text{Re}(I_\omega - I_{-\omega})}{2} - i\pi \frac{|k^2 - (t + \omega)\omega|}{4\omega} \theta(\mu - \omega) [\theta(\rho_{t+\omega}^2) - \theta(-\rho_\omega^2)], \quad (\text{A17})$$

where $R_\omega = R_\omega^\epsilon + \tilde{R}_\omega$, $I_\omega = I_\omega^\epsilon + \tilde{I}_\omega$, and

$$R_\omega^\epsilon = i \frac{|k^2 + (t - \omega)\omega|}{2\omega} \left[\widehat{f}_{t-\omega}^\omega \left(\frac{-k^2}{\omega} \right) \Big|_{t-\omega+\epsilon}^{2\tilde{\mu}-\omega} + \widehat{f}_\omega^{t-\omega} \left(\frac{k^2}{\omega-t} \right) \Big|_{\omega+\epsilon}^{2\mu+\omega} - \widehat{f}_{t-\omega}^\omega \left(\frac{k^2}{\omega} \right) \Big|_{t+\omega}^{2\tilde{\mu}+\omega} - \widehat{f}_{-\omega}^{t-\omega} \left(\frac{k^2}{\omega-t} \right) \Big|_\omega^{2\mu+\omega} \right], \quad (\text{A18})$$

$$\tilde{R}_\omega = \widehat{v}_\omega \left(\frac{-k^2}{\omega} \right) \Big|_{t-\omega}^{2\tilde{\mu}-\omega} - \frac{3k^4 - k^2t^2 - 5k^2\omega^2 + 2\omega^4}{2(\omega^2 - k^2)} \widehat{u}_\omega \left(\frac{-k^2}{\omega} \right) \Big|_{t-\omega}^{2\tilde{\mu}-\omega} + [(\omega - t)^2 - k^2] \widehat{u}_{t-\omega} \left(\frac{k^2}{\omega - t} \right) \Big|_\omega^{2\mu+\omega}, \quad (\text{A19})$$

$$I_\omega^\epsilon = \frac{|k^2 + (t - \omega)\omega|}{2\omega} \left(\widehat{f}_{t-\omega}^\omega(-\omega) \Big|_{t+\omega}^{2\tilde{\mu}+\omega} - \widehat{f}_{-\omega}^{t-\omega}(t - \omega) \Big|_\omega^{2\mu+\omega} - \widehat{f}_{t-\omega}^\omega(\omega) \Big|_{t-\omega+\epsilon}^{2\tilde{\mu}-\omega} + \widehat{f}_\omega^{t-\omega}(t - \omega) \Big|_{\omega+\epsilon}^{2\mu+\omega} \right), \quad (\text{A20})$$

$$\tilde{I}_\omega = \widehat{v}_\omega(\omega) \Big|_{t-\omega}^{2\tilde{\mu}-\omega} - \frac{3k^4 - k^2t^2 - 5k^2\omega^2 + 2\omega^4}{2(\omega^2 - k^2)} \widehat{u}_\omega(\omega) \Big|_{t-\omega}^{2\tilde{\mu}-\omega} - [(\omega - t)^2 - k^2] \widehat{u}_{t-\omega}(t - \omega) \Big|_\omega^{2\mu+\omega}. \quad (\text{A21})$$

Here

$$\rho_\omega = \sqrt{k^2 \frac{\omega^2 - k^2 - t^2}{\omega^2 - k^2}}, \quad \tilde{\mu} = \mu + t/2, \quad f_\Omega^\omega(r) = \tan^{-1} \left(\frac{e^{i \sin^{-1}(r/\rho_\omega)} - i\Omega/\rho_\omega}{\sqrt{\Omega^2/\rho_\omega^2 - 1}} \right), \quad \tilde{f}_\Omega^\omega(r) = \text{sgn}[\omega(\omega^2 - k^2 - t^2)] f_\Omega^\omega(r) \quad (\text{A22})$$

and

$$v_\omega(x) = \frac{x\sqrt{\rho_\omega^2 - x^2}}{4\sqrt{k^2 - \omega^2}}, \quad \tilde{v}_\omega(x) = \text{sgn}[\omega(k^2 - \omega^2)]v_\omega(x), \quad u_\omega(x) = \frac{\sin^{-1}(x/\rho_\omega)}{4\sqrt{k^2 - \omega^2}}, \quad \tilde{u}_\omega(x) = \text{sgn}[\omega(k^2 - \omega^2)]u_\omega(x). \quad (\text{A23})$$

Expression (A17) should be understood in the limit $\epsilon \rightarrow 0$. Taking this limit explicitly, we find

$$\begin{aligned} \Pi^-(\omega, k) = & -\mu + \frac{\text{Re}(R_\omega^{\text{reg}} + R_{-\omega}^{\text{reg}} + \tilde{R}_\omega + \tilde{R}_{-\omega})}{2} + i \frac{\text{Re}(I_\omega^{\text{reg}} - I_{-\omega}^{\text{reg}} + \tilde{I}_\omega - \tilde{I}_{-\omega})}{2} - i\pi \frac{|k^2 - (t + \omega)\omega|}{4\omega} \left(\theta(\mu - \omega) \left\{ \theta[\rho_{t+\omega}^2] \right. \right. \\ & \left. \left. - \theta(-\rho_\omega^2) \right\} - \frac{\pi}{2} \theta(\omega^2 - k^2 - t^2) \right) - i\pi \frac{|k^2 - (t - \omega)\omega|}{4\omega} \theta[(\omega - t)^2 - \omega^2 - k^2], \end{aligned} \quad (\text{A24})$$

where

$$\begin{aligned} R_\omega^{\text{reg}} = & i \frac{|k^2 + (t - \omega)\omega|}{2\omega} \left(\tilde{G}_{\omega, t-\omega}^{2\tilde{\mu}-\omega, -k^2/\omega} - \tilde{G}_{\omega, t-\omega}^{2\tilde{\mu}+\omega, k^2/\omega} + \tilde{G}_{\omega, t-\omega}^{t+\omega, k^2/\omega} + \tilde{G}_{t-\omega, \omega}^{2\mu+\omega, k^2/(\omega-t)} - \tilde{G}_{t-\omega, -\omega}^{2\mu+\omega, k^2/(\omega-t)} + \tilde{G}_{t-\omega, -\omega}^{\omega, k^2/(\omega-t)} \right) \\ & + \frac{k^2 + (t - \omega)\omega}{2\omega} \left(i \text{sgn}(\omega) \tilde{f}_{t-\omega}^\omega \left(\frac{-k^2}{\omega} \right) - \frac{1}{2} \ln \mu \frac{\sqrt{\rho_\omega^2 - (t - \omega)^2} + i(t - \omega)}{\rho_\omega^2 - (t - \omega)^2} + (\omega \rightarrow t - \omega) \right), \end{aligned} \quad (\text{A25})$$

$$\begin{aligned} I_\omega^{\text{reg}} = & \frac{|k^2 + (t - \omega)\omega|}{2\omega} \left(G_{\omega, t-\omega}^{2\tilde{\mu}+\omega, -\omega} - G_{\omega, t-\omega}^{t+\omega, -\omega} - G_{t-\omega, -\omega}^{2\mu+\omega, t-\omega} + G_{t-\omega, -\omega}^{\omega, t-\omega} - G_{\omega, t-\omega}^{2\tilde{\mu}-\omega, \omega} + G_{t-\omega, \omega}^{2\mu+\omega, t-\omega} \right) \\ & + \frac{|k^2 + (t - \omega)\omega|}{2\omega} \left[\theta(k^2 - \omega^2) \cos^{-1} \left(\frac{t - \omega}{\rho_\omega} \right) - \frac{\pi}{2} \theta(-\rho_\omega^2) - f_{t-\omega}^\omega(\omega) + (\omega \rightarrow t - \omega) \right], \end{aligned} \quad (\text{A26})$$

and

$$G_{\omega, \Omega}^{a, b} = \text{sgn}(b - a) [f_\Omega^\omega(b) - f_\Omega^\omega(a)], \quad \tilde{G}_{\omega, \Omega}^{a, b} = \text{sgn}(b - a) [\tilde{f}_\Omega^\omega(b) - \tilde{f}_\Omega^\omega(a)]. \quad (\text{A27})$$

In the weak-coupling limit $t \rightarrow 0$, we have the following expression:

$$\Pi^-(\omega, k) = -\mu + \frac{\text{Re}(R_\omega^{t=0} + R_{-\omega}^{t=0}) + i \text{Re}(I_\omega^{t=0} - I_{-\omega}^{t=0})}{2}, \quad (\text{A28})$$

$$R_\omega^{t=0} = \frac{\text{sgn}[(k^2 - \omega^2)(k^2 - \omega^2 + 2\omega\mu)]((2\mu - \omega)\sqrt{k^2 - (2\mu - \omega)^2} + k^2\{\sin^{-1}(k/\omega) - \sin^{-1}[(\omega - 2\mu)/k]\})}{4\sqrt{k^2 - \omega^2}}, \quad (\text{A29})$$

$$I_\omega^{t=0} = \text{sgn}(\mu - \omega) \left(\frac{(2\mu - \omega)\sqrt{k^2 - (2\mu - \omega)^2}}{4\sqrt{k^2 - \omega^2}} - \frac{k^2\{\sin^{-1}[(\omega - 2\mu)/k] + \sin^{-1}(\omega/k)\}}{4\sqrt{k^2 - \omega^2}} - \frac{\omega}{4} \right). \quad (\text{A30})$$

We can unite real and imaginary parts in one expression:

$$\Pi^-(\omega, k) = -\mu - \frac{t(k^2 - 2\omega^2)}{2(\omega^2 - k^2)} + \frac{P_\omega + \overline{P_{-\omega}}}{4}, \quad (\text{A31})$$

where

$$\begin{aligned} P_\omega = & G_{\omega+t} - \frac{3k^4 - k^2(t^2 + 5\omega^2) + 2\omega^4}{2(\omega^2 - k^2)^2} G_\omega + i \frac{\mu_\star}{2} \sqrt{\frac{\rho_\omega^2 - \mu_\star^2}{\omega^2 - k^2}} + i0 \frac{k^2 + \omega\mu_\star}{\omega^2 - k^2} + \frac{Q_{-\omega}^{\mu_\star} - Q_{+\omega-t}^{\omega-2\mu} + Q_{-\omega-t}^{2\mu-\omega} - Q_{-\omega}^{\mu_\star}}{2\omega} \\ & + \frac{k^2 - \omega(t + \omega)}{2\omega} \ln \frac{\rho_\omega^2 \mu_\star^2 [(\omega^2 - k^2)[\omega(\omega + 2t) - k^2]}{[k^2 - \omega(\omega + t)]^4} + \frac{i\pi |k^2 - \omega(t + \omega)|}{2\omega} \{ \theta[\omega^2 - k^2 - t^2] - \theta[\omega(\omega + 2t) - k^2] \}, \end{aligned} \quad (\text{A32})$$

and the functions G_ω and $Q_{\pm, \omega}^r$ are determined in Eqs. (2.20)–(2.22).

*gamayun@bitp.kiev.ua

¹K. S. Novoselov, A. K. Geim, S. V. Morozov, D. Jiang, Y. Zhang, S. V. Dubonos, I. V. Grigorieva, and A. A. Firsov, *Science* **306**, 666 (2004).

²G. W. Semenoff, *Phys. Rev. Lett.* **53**, 2449 (1984); P. R. Wallace, *Phys. Rev.* **71**, 622 (1947).

³V. N. Kotov, B. Uchoa, V. M. Pereira, A. H. Castro Neto, and F. Guinea, e-print [arXiv:1012.3484](https://arxiv.org/abs/1012.3484).

- ⁴S. Das Sarma, S. Adam, E. H. Hwang, and E. Rossi, *Rev. Mod. Phys.* **83**, 407 (2011).
- ⁵Ed. McCann and V. I. Fal'ko, *Phys. Rev. Lett.* **96**, 086805 (2006).
- ⁶E. H. Hwang and S. Das Sarma, *Phys. Rev. Lett.* **101**, 156802 (2008).
- ⁷R. Nandkishore and L. Levitov, *Phys. Rev. Lett.* **104**, 156803 (2010).
- ⁸E. V. Gorbar, V. P. Gusynin, and V. A. Miransky, *JETP Lett.* **91**, 314 (2010).
- ⁹E. V. Gorbar, V. P. Gusynin, and V. A. Miransky, *Phys. Rev. B* **81**, 155451 (2010).
- ¹⁰O. V. Gamayun, E. V. Gorbar, and V. P. Gusynin, *Phys. Rev. B* **81**, 075429 (2010).
- ¹¹J. Gonzalez, e-print [arXiv:1103.3650](https://arxiv.org/abs/1103.3650).
- ¹²G. Borghi, M. Polini, R. Asgari, and A. H. MacDonald, *Solid State Commun.* **149**, 1117 (2009).
- ¹³G. Borghi, M. Polini, R. Asgari, and A. H. MacDonald, *Phys. Rev. B* **80**, 241402 (2009).
- ¹⁴S. V. Kusminskiy, J. Nilsson, D. K. Campbell, and A. H. Castro Neto, *Europhys. Lett.* **85**, 58005 (2009).
- ¹⁵B. Wunsch, T. Stauber, F. Sols, and F. Guinea, *New. J. Phys.* **8**, 318 (2006).
- ¹⁶E. H. Hwang and S. Das Sarma, *Phys. Rev. B* **75**, 205418(2007).
- ¹⁷R. Sensarma, E. H. Hwang, and S. Das Sarma, *Phys. Rev. B* **82**, 195428 (2010).
- ¹⁸P. K. Pyatkovskiy, *J. Phys.: Condens. Matter* **21**, 025506 (2009).
- ¹⁹A. Qaiumzadeh and R. Asgari, *Phys. Rev. B* **79**, 075414 (2009).
- ²⁰K. Shizuya, *Phys. Rev. B* **75**, 245417 (2007).
- ²¹R. Roldan, J.-N. Fuchs, and M. O. Goerbig, *Phys. Rev. B* **80**, 085408 (2009).
- ²²R. Roldan, J.-N. Fuchs, and M. O. Goerbig, *Semicond. Sci. Technol.* **25**, 034005 (2010).
- ²³P. K. Pyatkovskiy and V. P. Gusynin, *Phys. Rev. B* **83**, 075422 (2011).
- ²⁴V. P. Gusynin, S. G. Sharapov, and J. P. Carbotte, *Int. J. Mod. Phys. B* **21**, 4611 (2007).
- ²⁵E. V. Gorbar, V. P. Gusynin, V. A. Miransky, and I. A. Shovkovy, *Phys. Rev. B* **66**, 045108 (2002).
- ²⁶S. Yuan, R. Roldan, and M. I. Katsnelson, e-print [arXiv:1103.5350](https://arxiv.org/abs/1103.5350), *Phys. Rev. B* (to be published).
- ²⁷Xue-Feng Wang and Tapash Chakraborty, *Phys. Rev. B* **75**, 041404(R) (2007).
- ²⁸Really $T \sum_{n=-\infty}^{\infty} (i\Omega_n - \mu + a)^{-1} (i\Omega_n - \mu + b)^{-1} = [n_F(a) - n_F(b)] / (a - b)$ where $n_F(x) = \{1 + \exp[(x - \mu)/T]\}^{-1}$.
- ²⁹In the weak coupling regime, the number of flavours effectively doubles.
- ³⁰One can easily see that $\hat{f}(x)_a^b = \int_a^b dr f'(r) \text{sgn}(r - x)$.